

# Introduction

Estimates of extension in the Basin and Range range are commonly above 100 percent (Hamilton, 1978; Wernicke et. al, 1988; Proffett, 1977). Examination of earthquake mechanisms in the western United States reveals the complete absence of large events occurring on normal faults with dips less than 38° (Doser and Smith, 1989). A global study by Jackson (1987) shows a similar limit (approximately 35°) on normal fault dip and reveals that faults are essentially planar and dip steeply down to the brittle-ductile transition. As well, frictional constraints have been used to argue that it is more favorable to create new, steeply-dipping faults than accumulate slip on low-angle normal faults.

Given planar faults and minimum fault dip of 38°, simple geometric relations (Jackson and McKenzie, 1983) can be used to show that the maximum extension possible from a single fault system with rotation of dip is 40%. Beyond 40%, extension must be taken up by a new set of high-angle faults cutting the old system, or by aseismic slip on faults which have rotated to a low angle.

In contrast, several researchers have compiled observations to argue for the existence of Quaternary seismic slip on low-angle normal faults (Axen et al., 1998; Abers, 1983; Burchfiel et al., 1987; Johnson and Loy, 1992). Also, it has been shown that it is energetically more feasible to accommodate large amounts extension on normal faults of low dip (Forsyth, 1992).

Here, we present the results of a seismic reflection and gravity experiment to test whether or not part of the 16 December 1954 Dixie Valley Earthquake (Ms=6.8) produced slip on a low-angle normal fault.

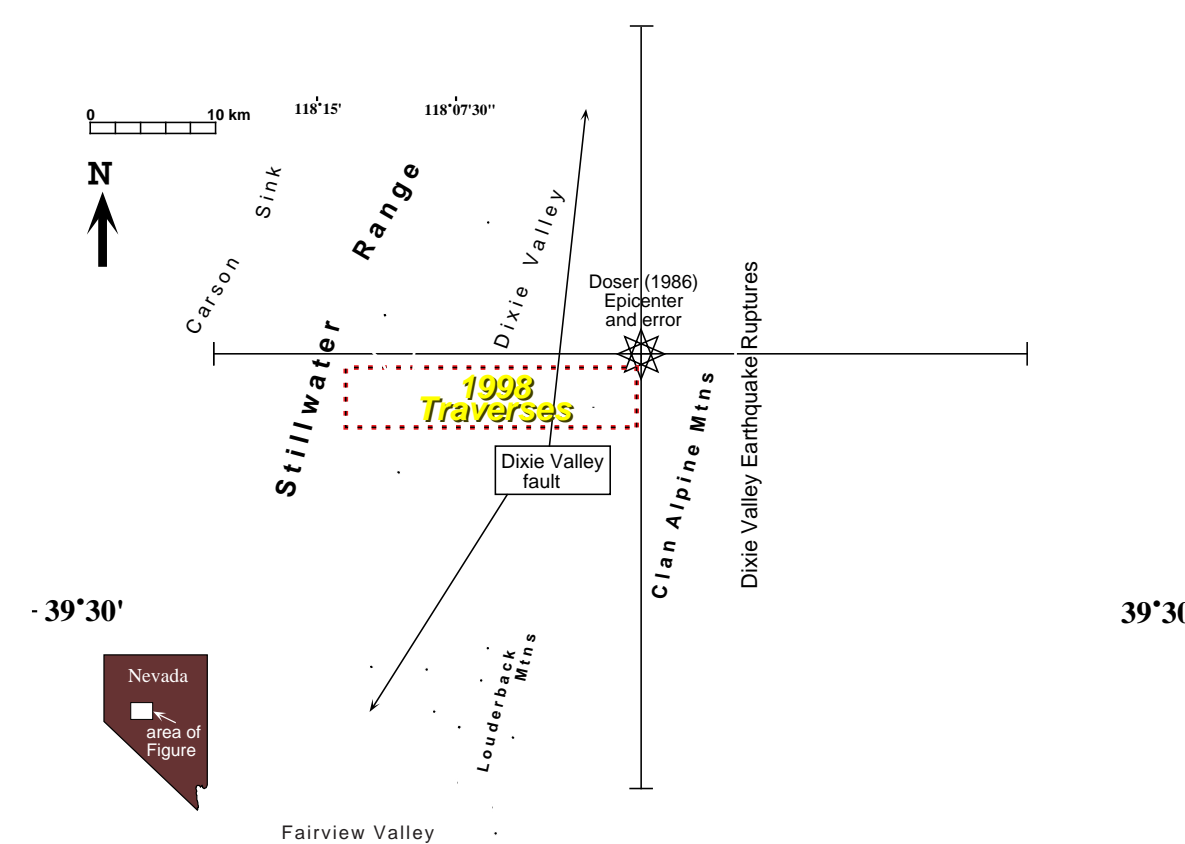


**Fig. 1: Dixie Valley Rupture Map**

Map of Dixie Valley in central Nevada. The extent of the 1954 Dixie Valley surface rupture is denoted by the white arrow. The large error estimate in the epicenter location is a result of contamination of the waveforms by the nearby Fairview Peak (Ms=7.2) earthquake, four minutes in advance. There is a correspondingly large error in fault dip determination.

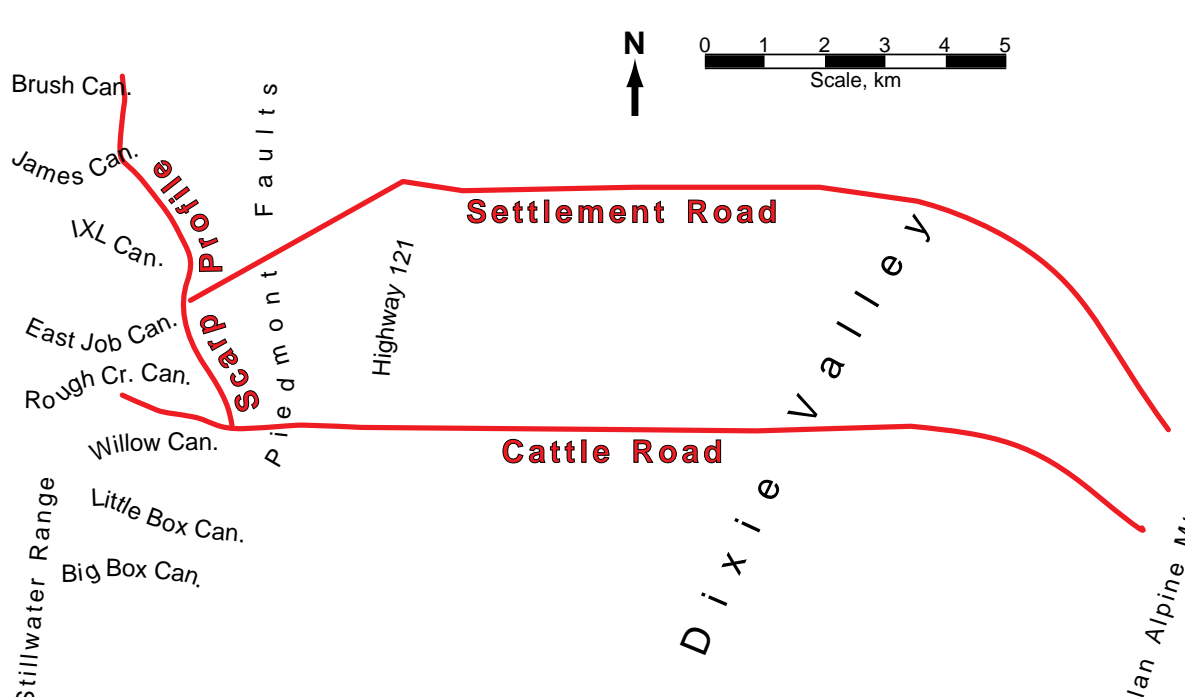


**Fig. 2: 1998 Traverses**

This figure shows the location of our 1998 geophysical field work. High- and medium-resolution seismic reflection profiles were conducted along Cattle Road from the range-front scarp eastward. Gravity transects were conducted across the valley along Settlement and Cattle Roads and along the scarp from Willow Canyon to Brush Canyon.

# Field Acquisition and Data Reduction Methods

**Fig. 3: Seismic Data Acquisition**

This is a view of Dixie Valley near the fault scarp and looking east, along Cattle Road. Receiver locations for the medium-resolution survey are red flags. The medium-resolution profile utilized 8 Hz geophones, explosives at 2 m depth, and extended 3.6 km into the basin. It was composed of 4 stationary setups of 48 receivers with 15.2 meter spacing. The high-resolution profile was conducted within 130 m of the range-front scarp with 100 Hz geophone groups, 2 m spacing, and a sledgehammer source. A linear array of 6 geophones per group was used to reduce ground-roll in the high-resolution survey. In both surveys, off-end and longer-offset shots were recorded to increase fold and gather deep velocity information.

1954 Picture of Range-Front Scarp, East Job Canyon Photo by Karl V. Steinbrugge

**Fig. 4: Gravity Data Acquisition**

Gravity measurements were made with a LaCoste & Romberg Model G gravity meter. Vertical control is supplied by a Trimble geodetic-quality GPS. Data were reduced to simple Bouguer anomaly with a 2.67 g/cc reduction density and innering terrain corrections to 100 m. Additional data from Schaefer's (1984) gravity study were incorporated to increase station density.

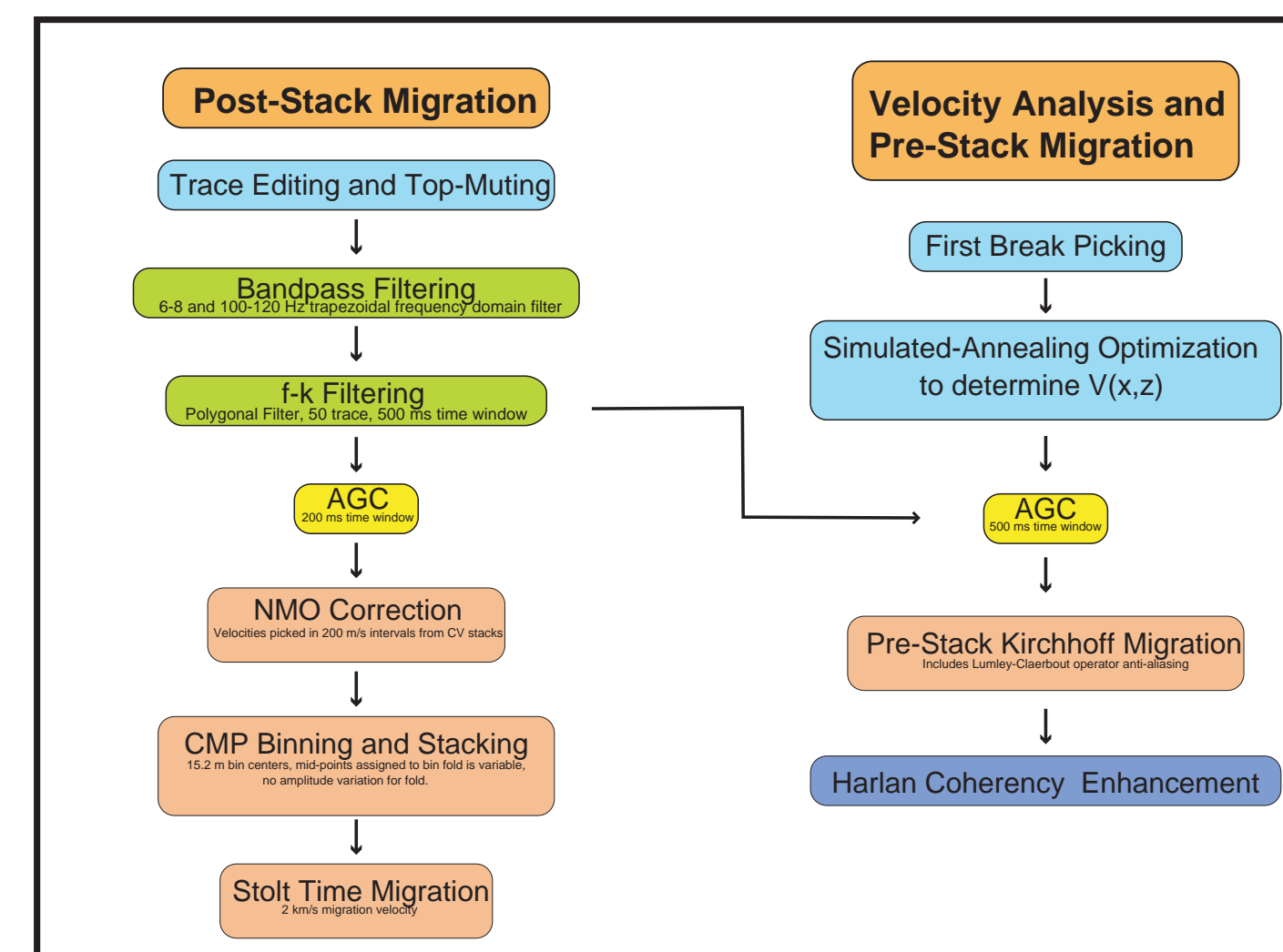


**Fig. 5: Processing Flows**

# Velocity Analysis and Acoustical Modeling

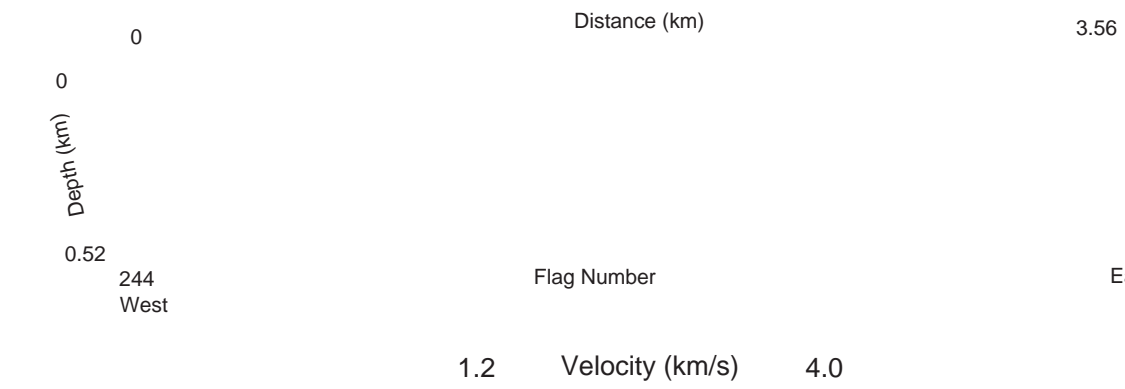


**Fig. 6: 3-D Velocity Model**

This is a velocity model obtained from a simulated-annealing non-linear optimization of first arrival picks (Pullammanappillil and Louie, 1994). A three-dimensional inversion was calculated because of a slightly crooked-line geometry along the Cattle Road profile. The 3-D model was subsequently "flattened" to 2-D for use in Kirchhoff pre-stack migration as in (Chavez-Perez, et al., 1998.)

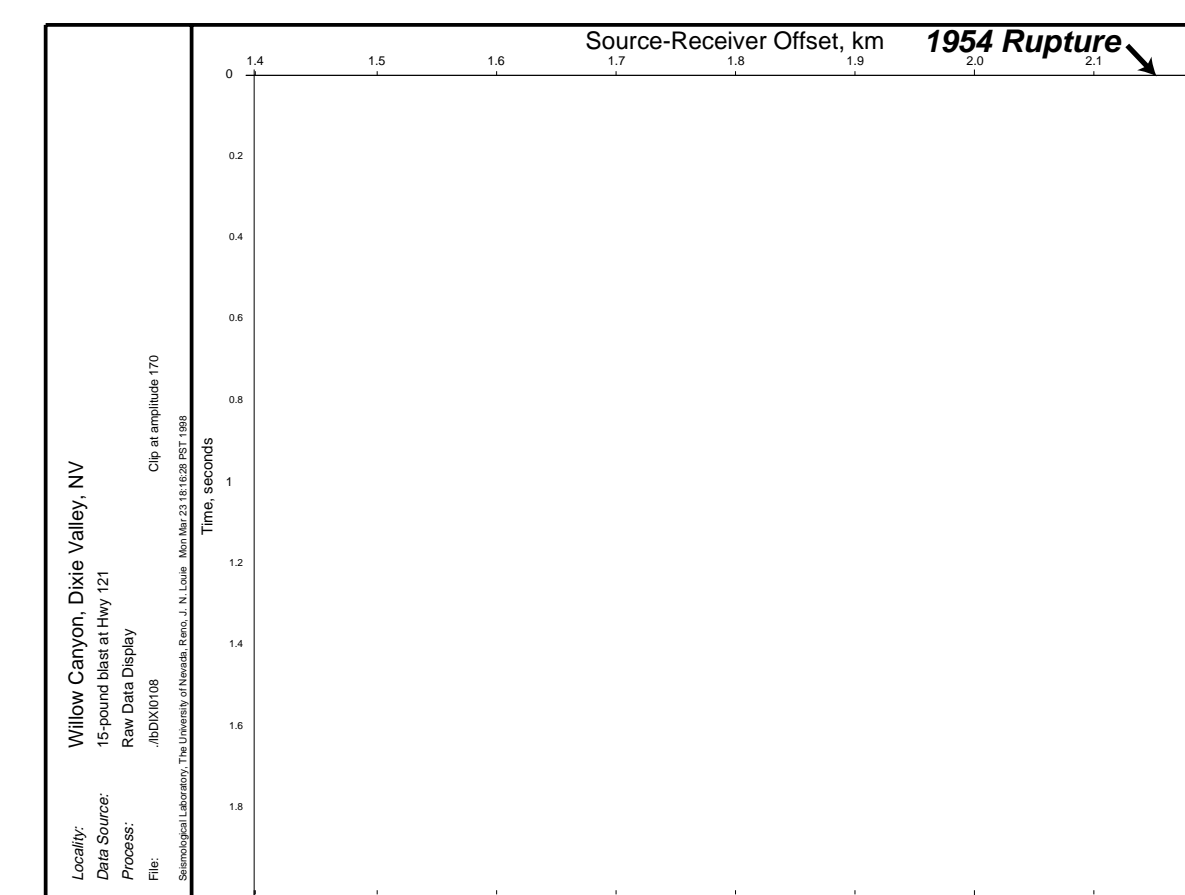


**Fig. 7: Refraction Experiment**

This raw, long-offset shot gather from our medium-resolution profile shows a headwave propagating vertically from the fault surface (highlighted). The coincident first-arrivals across the entire receiver array limit the range of the dip of the fault. The shot geometry and interpretation is given in Figure 8.

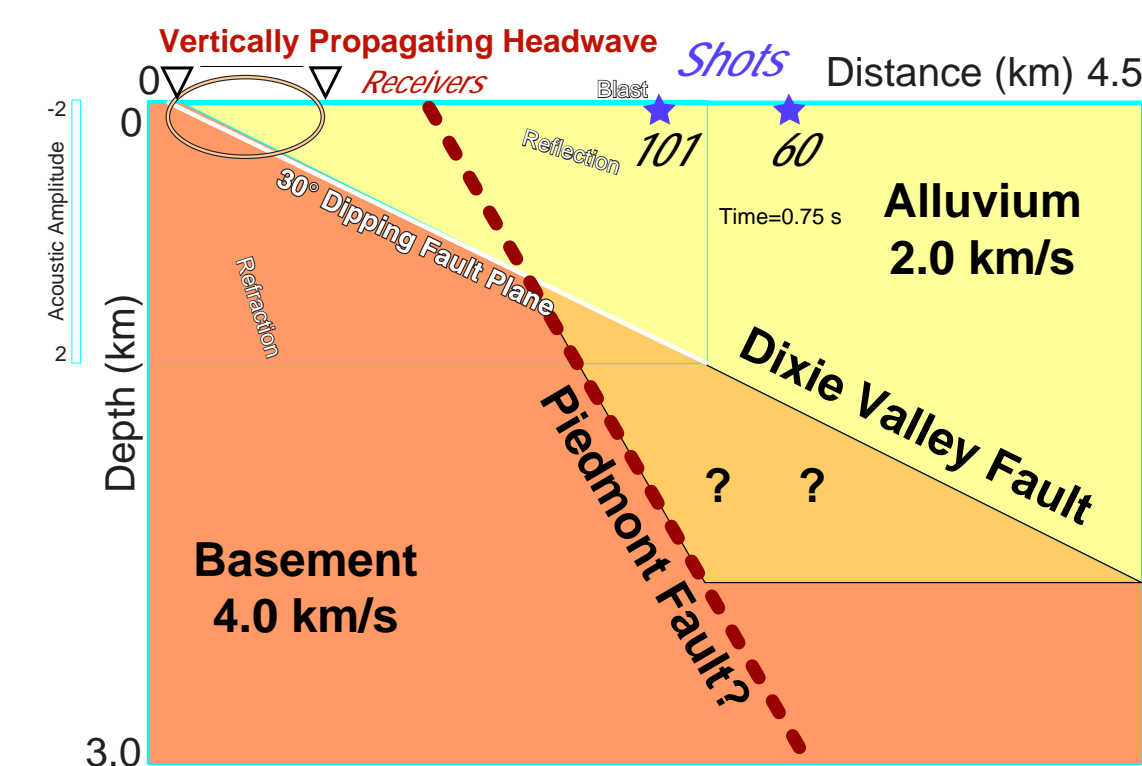


**Fig. 8: Acoustic Model of Headwave**

This is an acoustic model of the vertically propagating headwave shown in Figure 7. The model assumes a basement-alluvium velocity contrast of 2 to 1, along a 30° dipping fault plane. The array of receivers is shown near the fault scarp. Energy from the blast, at flag number 101 (2.1 km), reflects and refracts off the fault interface. This geometry reproduces the vertically propagating headwave seen on the shot record. Similar refractions along the high-resolution seismic line (not shown) demonstrate that the fault plane continues along this dip to the surface. The synthetics were produced by a finite-difference solution to the scalar wave equation described by HelMBERGER and VIDALE (1988).

# Results

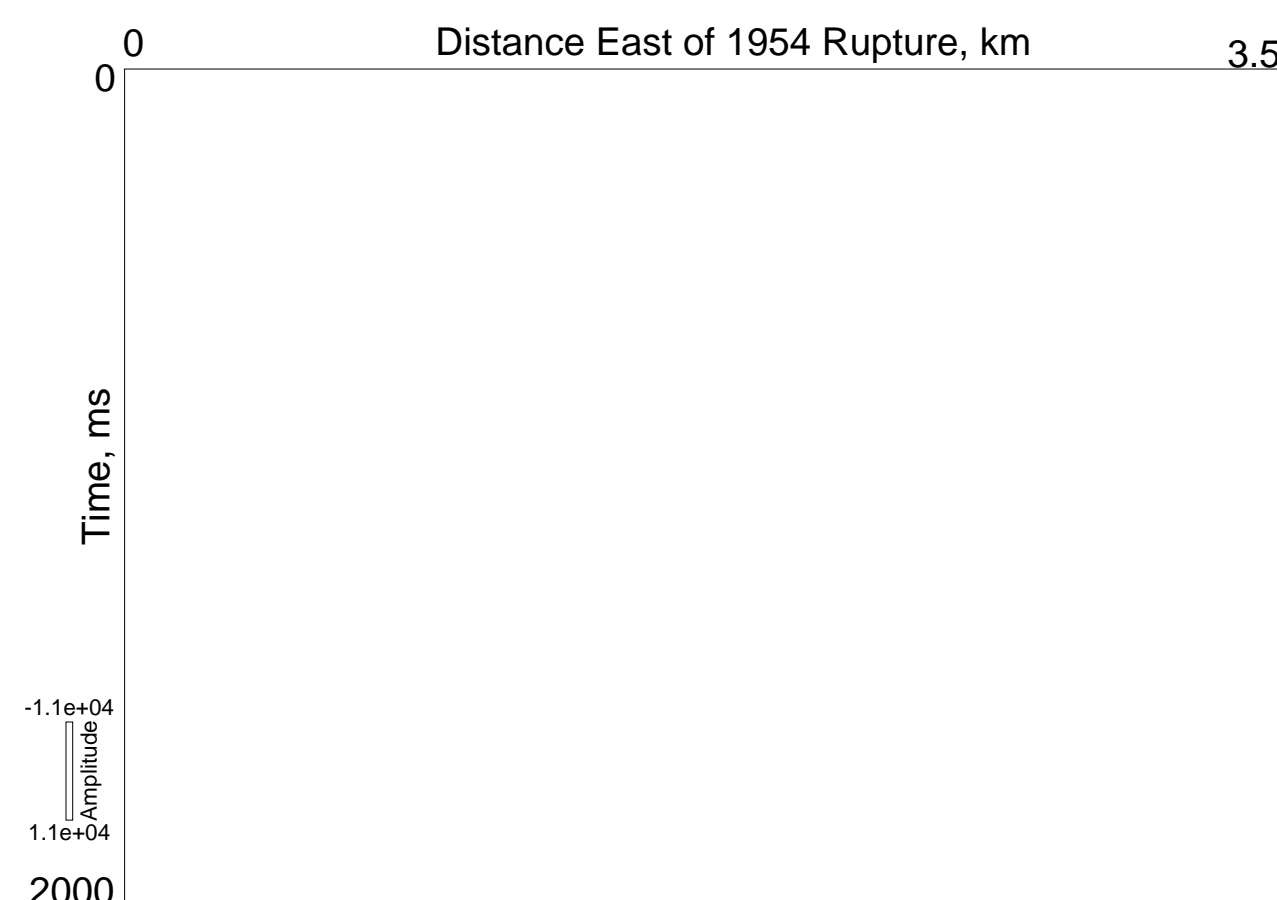


**Fig. 9: 2.0 km/s Stolt-Migrated Stack**

This is a post-migrated stack of our medium-resolution Cattle Road profile, following the processing flow given in figure 5. The fault plane reflector, dipping eastward at 25-30°, can be traced to its surface outcrop. Reflections sub-parallel to the fault can be seen in the footwall, suggesting foliation in the granite. Highly reflective Tertiary basalt layers in the hanging wall begin to obscure the fault reflections at about 500 ms. However, the basalt layers can be traced to the extension of the fault at depth, where they are seen to terminate, after forming small roll-over anticlines. The roll-over anticlines support a listric fault geometry.

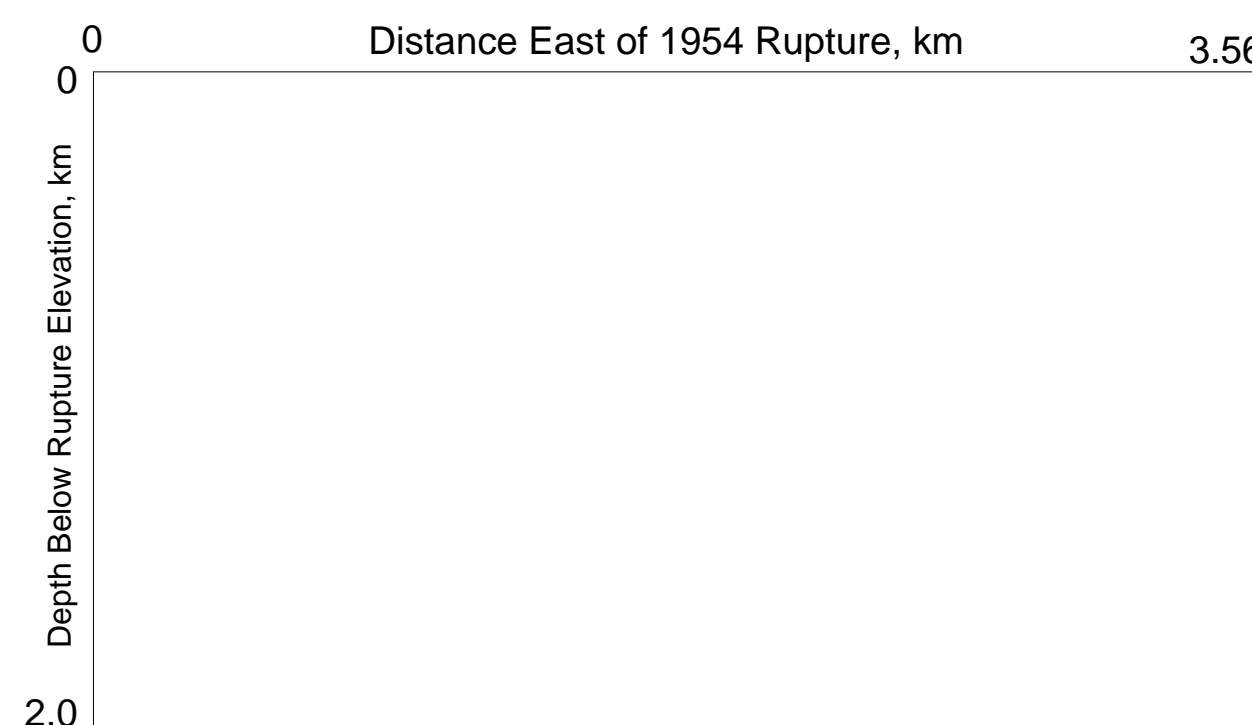


**Fig. 10: Enhanced, Anti-Aliased Pre-Stack Migration**

This is a pre-stack migration of the same profile as above, also following the flow given in figure 5. The migration used the Lumley-Claerbout operator anti-aliasing criterion, yielding a longer-wavelength view of subsurface reflectivity. With it, we can see below the reflective basalts in the hanging wall, and image the shallowly-dipping fault to 1.5 km depth.

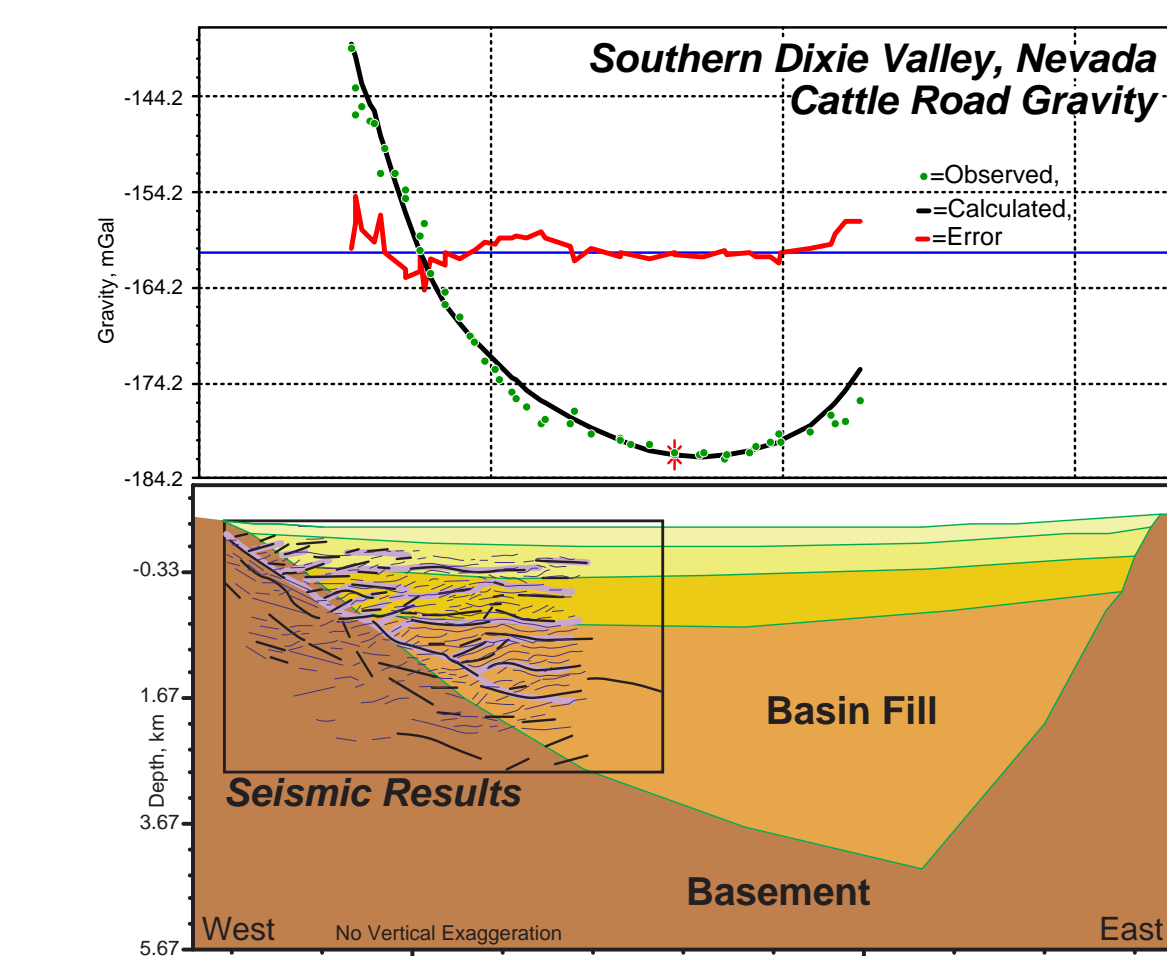


**Fig. 11: Preliminary Gravity Basin Model**

This is a modeled basin geometry of the gravity data obtained along the Cattle Road Profile. The scatter in the observed points is due to insufficient elevation control as the roving-mode GPS data has yet to be fully rectified. Even so, the shape of the anomaly is not affected by the scatter and it is compatible with a low-angle geometry. A 1:1 overlay of the seismic results is consistent with the low-angle hypothesis. The gradational density in the basin fill follows a regional scheme used by Blakely et al. (1996) in their gravity inversions. Modeling was done with the GM-SYS package by Northwest Geophysical Associates.

# Conclusions

Our results indicate that slip along a section of the 16 December 1954 Dixie Valley earthquake rupture took place along a fault plane of unusually low dip (25-30°). In this regard, it is the first large historical earthquake for which slip on a low-angle normal fault has been documented.

## Selected References

Abers, G. A., 1991, Possible seismogenic shallow-dipping normal faults in the Woodlark-D'Entrecasteaux extensional province, Papua New Guinea: *Geology*, **19**, 1205-1208.

Axen, G. J., J. M. Fletcher, E. Cowgill, M. Murphy, P. Kapp, I. MacMillan, E. Ramos-Velazquez, and J. Aranda-Gomez, 1998, Range-front fault scarps of the Sierra El Mayor, Baja California: Formed above and active low-angle normal fault?: in submission *Geology*.

Blakely, R. J., R. C. Jachens, J. P. Calzia, and V. E. Langenheim, 1996, Cenozoic basins of the Death Valley extended terrain as reflected in regional-scale gravity anomalies: in submission *GSA Spec. Pub.*.

Burchfiel, B. C., K. V. Hodges, and L. H. Royden, 1987, Geology of Panamint Valley-Saline Valley pull-apart system, California: Palinspatic evidence for low-angle geometry of a Neogene range-bounding fault: *J. Geophys. Res.*, **92**, 10,422-10,426.

Caskey, S. J., S. G. Wesnousky, P. Zhang, and D. B. Slemmons 1996, Surface faulting of the 1954 Fairview Peak (Ms 7.2) and Dixie Valley (Ms 6.8) earthquakes, Central Nevada: *Bull. Seis. Soc. Am.*, **86**, 761-787.

Chavez-Perez S., J. N. Louie, and S. K. Pullammanappillil, 1998, Seismic depth imaging of normal faulting in the southern Death Valley basin: *Geophysics*, **63**, 223-23097-1409.

Doser, D. I., and R. B. Smith, 1989, An assessment of source parameters of earthquakes in the cordillera of the western United States, *Bull. Seis. Soc. Am.*, **79**, 1383-1409.

Forsyth, D. W., 1992, Finite extension and low-angle normal faulting: *Geology*, **20**, 27-30.

Hamilton, W., 1978, Mesozoic tectonics of the western United States, in Howell, D. G., et al., Eds, Mesozoic paleogeography of the western United States: *Soc. Ec. Paleontologists and Mineralogists, Pacific Coast Paleogeography Symp.*, 33-70.

HelMBERGER, D. V., and J. E. VIDALE, 1988, Modeling strong motions produced by earthquakes with two-dimensional numerical codes: *Bull. Seis. Soc. Am.*, **78**, 109-121.

Jackson, J., and D. McKenzie, 1983, The geometrical evolution of normal fault systems: *J. Struct. Geol.*, **5**, No. 5, 471-482.

Jackson, J. A., 1987, Active normal faulting and extension: in Coward, M. P. et al. Eds, *Continental Extensional Tectonics*, *Geol. Soc. Am. Spec. Pub.*, **28**, 3-17.

Johnson, R. A., and K. L. Loy, 1992, Seismic reflection evidence for seismogenic low-angle faulting in southeastern Arizona: *Geology*, **20**, 597-600.

Lumley, D. C., D. Claerbout, 1994, Anti-aliased Kirchhoff 3-D migration: *Expanded Abstracts, Soc. Explor. Geoph., Ann. Internat. Mtg., Los Angeles*

Proffett, J. M., Jr., 1977, Cenozoic geology of the Yerington district, Nevada, and implications for the nature and origin of Basin and Range faulting: *Geol. Soc. Am. Bull.*, **88**, 247-266.

Pullammanappillil, S. K., and J. N. Louie, 1994, A generalized simulated-annealing optimization for inversion of first-arrival times: *Bull. Seismo. Soc. Amer.*, **84**, 1397-1409.

Schaefer, D. H., J. M. Thomas, B. G. Duffrin, 1983, Gravity survey of Dixie Valley, west-central Nevada: *USGS OFR 82-111, 17 p.*

Wernicke, B., 1995, Low-angle normal faults and extension: A review: *J. Geophys. Res.*, **100**, No. B10, 20,159-20,174.

Wernicke, B., G. L. Axen, and J. K. Snow, 1988, Basin and Range extensional tectonics at the latitude of Las Vegas, Nevada: *Geol. Soc. Am. Bull.*, **100**, 1738-1757.

## Acknowledgements

This project was funded by the National Science Foundation (EAR-9706255). The W. M. Keck Foundation donated seismic equipment, computers, and modeling software. All geophysical fieldwork was performed by the spring 1998 Geophysical Applications class at the University of Nevada, Reno. Class participants were: Ana Cadena, Travis Rabe, Matt Herrick, Mandy Johnson, Andrew Rael, Tom Blechen, and Evan Hobson. Additional field assistance was rendered by Christine Mann, Jim Ollerton, and John Oswald. Simulated-annealing of first-arrival picks was performed by Sathish Pullammanappillil of OPTIM L. L. C.. Thanks to Mike Dennis and Nevada Precision Drilling and Blasting for their work. We also thank Prill Meacham and the Carson City office of the BLM for their assistance and cooperation.